Crystal structure of human copper homeostasis protein CutC reveals a potential copper-binding site

ARTICLE *in* JOURNAL OF STRUCTURAL BIOLOGY · OCTOBER 2009

Impact Factor: 3.23 · DOI: 10.1016/j.jsb.2009.10.012 · Source: PubMed

4 AUTHORS, INCLUDING:

Peng Zhang
Institute of Plant Physiology and Ecology
18 PUBLICATIONS **276** CITATIONS
SEE PROFILE

Jianping Ding
Chinese Academy of Sciences
142 PUBLICATIONS **7,774** CITATIONS
SEE PROFILE

Journal of Structural Biology 169 (2010) 399–405

Contents lists available at ScienceDirect

Journal of Structural Biology

journal homepage: www.elsevier.com/locate/yjsbi

Crystal structure of human copper homeostasis protein CutC reveals a potential copper-binding site

Yingjie Li [a,b], Jiamu Du [a], Peng Zhang [a], Jianping Ding [a,*]

[a] State Key Laboratory of Molecular Biology and Research Center for Structural Biology, Institute of Biochemistry and Cell Biology, Shanghai Institutes for Biological Sciences, Chinese Academy of Sciences, 320 Yue-Yang Road, Shanghai 200031, China
[b] Graduate School of the Chinese Academy of Sciences, 320 Yue-Yang Road, Shanghai 200031, China

ARTICLE INFO

Article history:
Received 9 September 2009
Received in revised form 21 October 2009
Accepted 22 October 2009
Available online 28 October 2009

Keywords:
Copper homeostasis protein
CutC
Conserved sequence motif
Metal-binding site
Crystal structure

ABSTRACT

Copper is an essential trace element to life and particularly plays a pivotal role in the physiology of aerobic organisms. The Cut protein family is associated with copper homeostasis and involved in uptake, storage, delivery, and efflux of copper. CutC is a member of the Cut family and is suggested to be involved in efflux trafficking of cuprous ion. We report here the biochemical and structural characterization of human CutC (hCutC). hCutC can bind Cu(I) with a stoichiometry of 1:1 and an apparent dissociation constant of 15.5 ± 2.8 μM. hCutC assumes a typical TIM-barrel fold and forms a tetramer in both crystal structure and solution which is different from the dimeric architecture of the bacterial CutC. Structure analysis and sequence comparison of CutC proteins from different species reveal two strictly conserved Cys residues on the inner surface of the C-terminal end of the TIM-barrel. Mutations of the two Cys residues can significantly impair the binding ability of hCutC with Cu(I). Our results suggest that hCutC functions as an enzyme with Cu(I) as a cofactor rather than a copper transporter and the potential Cu(I)-binding site consists of the two Cys residues and other conserved residues in the vicinity.

1. Introduction

Copper is a trace metal element essential to all organisms which can act as a cofactor for many enzymes involved in redox reactions and various biological processes, including electron transfer in cytochrome, neuropeptides modification, and detoxification by Cu–Zn superoxide dismutase, etc. (Lee et al., 2001; Rensing and Grass, 2003). Copper homeostasis is strictly and precisely controlled to prevent copper accumulation beyond cellular needs because excessive copper is highly toxic to cells and can lead to cell death through binding to some essential cellular components (Pena et al., 1999). Disturbed copper homeostasis has been implicated in several genetic diseases in both human beings and animals including Menkes disease and Wilson disease (DiDonato and Sarkar, 1997; Schaefer and Gitlin, 1999).

So far, several gene families have been identified to be responsible for maintaining the balance of copper in cells. In bacteria, two gene families are involved in copper homeostasis from uptake to storage, delivery, and efflux (reviewed in Silver and Phung, 1996). One of them, the *cop* gene family, is well characterized and associated with uptake and export of copper. The other one, the *cut* gene family, is defined based on a preliminary characterization of copper-sensitive mutants. The *cut* gene family contains six members (*cut*A, *cut*B, *cut*C, *cut*D, *cut*E, and *cut*F) and has also been suggested to be involved in uptake, intracellular storage and transport, and efflux of copper. Among the *cut* members, *cut*C is conserved from bacteria to mammals. Mutation (Gupta et al., 1995) or deletion (Rensing and Grass, 2003) of *cut*C in *Escherichia coli* leads to increased copper sensitivity at high concentration of copper, probably due to a decreased efflux of copper (Gupta et al., 1995). Those results suggest that CutC may play an important role in intracellular trafficking of Cu(I) to alleviate the stress (Kimura and Nishioka, 1997; Rensing and Grass, 2003). In *Caenorhabditis elegans*, knockdown of *cut*C also increases the copper sensitivity and affects the worm phenotype at high level of copper (Calafato et al., 2008). To date, only the structure of CutC from *Shigella flexneri* (sfCutC) is described, which adopts a classical TIM-barrel fold and represents a new structural family of TIM-barrel (Zhu et al., 2005). However, the structure of sfCutC reveals very limited information about the biological function of CutC.

Human CutC (hCutC) is a cytoplasmic protein of 273 amino acid residues with a molecular mass of 30 kDa and is expressed ubiquitously in nearly all human tissues (Li et al., 2005; Ota et al., 2004). To gain insights into the potential function of hCutC, we carried out biochemical studies of hCutC and determined the crystal structure of hCutC at 2.5 Å resolution. The biochemical and structural data

Abbreviations: hCutC, human CutC; sfCutC, *Shigella flexneri* CutC.

* Corresponding author. Fax: +86 21 5492 1116.
E-mail address: jpding@sibs.ac.cn (J. Ding).

1047-8477/$ - see front matter © 2009 Elsevier Inc. All rights reserved.
doi:10.1016/j.jsb.2009.10.012

together suggest that hCutC is a Cu(I)-binding protein with a stoichiometry of 1:1 and an apparent dissociation constant of 15.5 ± 2.8 μM, and the potential Cu(I)-binding site consists of two strictly conserved Cys residues and other conserved residues nearby on the inner surface of the C-terminal end of the TIM-barrel. These results provide useful information for further functional analysis of hCutC.

2. Materials and methods

2.1. Cloning, expression, and purification

The *hCutC* gene (GenBank Accession No. NP_057044) was amplified by PCR from the cDNA library of human CD34 + haematopoietic stem/progenitor cells (Mao et al., 1998) and inserted into the *Sph*I and *Pst*I restriction sites of the expression vector pQE30 (Qiagen) which attaches a hexa-His tag at the N-terminus of the target protein. Plasmids encoding all mutant versions of hCutC were generated by site-directed mutagenesis using QuikChange kit (Stratagene). The wild-type hCutC in pQE30 vector was used as the template and the primers were designed to contain the desired mutations. All the mutations were verified by DNA sequencing.

The recombinant plasmids were transformed into *E. coli* strain DH5α (Novagen). The bacterial transformants were grown in LB medium and induced by 0.2 mM IPTG overnight at 18 °C. The bacterial cells were harvested by centrifugation at 4500 *g* and resuspended in the lysis buffer (20 mM Tris–HCl, pH 8.0, 500 mM NaCl, and 2 mM β-mercaptoethanol) supplemented with 1 mM phenylmethylsulfonyl fluoride. The cells were lysed on ice by sonication and the cell debris was removed by centrifugation at 15,000 *g* at 4 °C.

Protein purification was carried out by affinity chromatography at 4 °C. The supernatant was loaded onto an affinity chromatography column of nickel–nitrilotriacetic acid–agarose (Ni–NTA, Qiagen) pre-equilibrated with the lysis buffer and then washed with the lysis buffer supplemented with 10 mM imidazole. The target protein was eluted with the lysis buffer supplemented with 200 mM imidazole. The eluted sample was dialyzed against the dialysis buffer (20 mM Tris–HCl, pH 8.0, 100 mM NaCl, and 5 mM DTT) for three times. The purified protein was of sufficient purity (above 95%) as shown by SDS–PAGE analysis (Fig. 1A) and was then concentrated to about 10 mg/ml by ultra-filtration for further biochemical and structural studies.

2.2. Copper-binding analysis

The Cu(I)-binding assay was carried out using a method modified from that described previously (Jensen et al., 1999). Specifically, the protein was added into an aliquot of $CuCl_2$ solution containing 20 mM Hepes, pH 7.5, 150 mM NaCl, and 10 mM ascorbate. The concentration of $CuCl_2$ was varied from 0 to 250 μM, and the concentration of protein was maintained at 15 μM. Cu(II) was reduced to Cu(I) by ascorbate. When the reaction is completed, the unbound or non-specifically bound Cu(I) was removed by incubation of the solution with 60 mg of the cation-chelating resin Chelex 100 (Sigma) for 1 h. The concentration of the bound Cu(I) was determined spectrophotometrically using bicinchonic acid (BCA) (disodium salt, Sigma). To ensure that the Cu(I) ion bound with the protein was completely released to form the 2:1 BCA:Cu(I) complex, excessive amount of BCA (20 mM) was added to the sample and the amount of the formed BCA:Cu(I) complex was determined by measuring the absorbance of the mixture at 562 nm. The absorbance of the complex has a linear correlation with the Cu(I) concentration in accordance with the Beer–Lambert law. The protein concentration was re-assessed by the Bradford method

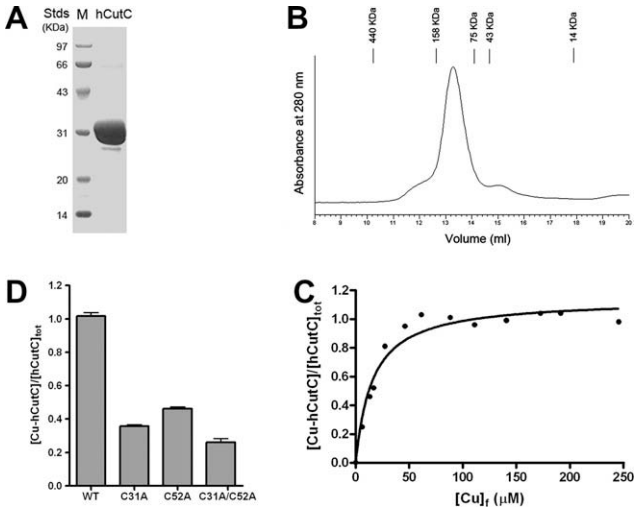

Fig. 1. Biochemical characterization of hCutC. (A) SDS–PAGE analysis of the purified recombinant hCutC. Positions of the molecular weight standards are marked. Below the target protein, there is a very weak band which could be an impurity or a degradation product of the target protein. (B) Analysis of the oligomeric state of hCutC in solution by size-exclusion chromatography. Absorbance at 280 nm is plotted against the elution volume. Positions of the molecular weight standards are indicated. (C) Cu(I)-binding analysis of hCutC. Lysozyme was served as a negative control. (D) The Cu(I)-binding abilities of the wild-type hCutC and the single mutants C31A and C52A and the double mutant C31A/C52A. All experiments were repeated at least three times and the error bars represent the standard deviation.

(Bio-Rad) using bovine serum albumin as a standard (Bradford, 1976). All experiments were repeated at least three times under the same condition.

The data were analyzed using the following equation which is derived from the mass law:

$$[\mathrm{Cu{-}hCutC}]/[\mathrm{hCutC}]_{\mathrm{tot}} = n \times [\mathrm{Cu}]_{\mathrm{f}}^{n_{\mathrm{H}}}/([\mathrm{Cu}]_{\mathrm{f}}^{n_{\mathrm{H}}} + K_{\mathrm{d}})$$

In the formula, $[\mathrm{hCutC}]_{\mathrm{tot}}$ is the total amount of protein, [Cu–hCutC] is the Cu(I) concentration bound to hCutC, and $[\mathrm{Cu}]_{\mathrm{f}}$ is the free Cu(I) concentration as determined by subtracting the bound Cu(I) concentration from the total Cu(I) concentration which is equivalent to the total $CuCl_2$ concentration initially added in the solution. K_{d} is the dissociation constant of hCutC with Cu(I), n is the number of binding sites, and n_{H} is the Hill coefficient. All the data were analyzed using the program Prism 4.0 (GraphPad software).

2.3. Crystallization and diffraction data collection

Crystallization conditions were screened with the Hampton Research Screens kits at 20 °C using the hanging-drop vapor-diffusion method. Crystals of hCutC were grown in drops containing equal volumes (1 μl) of the protein solution (10 mg/ml) and the reservoir solution (0.1 M citric acid, pH 4.0, and 10% (w/v) polyethylene glycol 6000) to a maximum size of 0.04 × 0.04 × 0.2 mm^3 in 2 weeks. Prior to data collection, we performed a fluorescence scan of the crystal in the wavelength range of 1.3507–1.4123 Å at synchrotron and no anomalous signal was detected at the wavelength of the Cu k-edge (λ = 1.38 Å), suggesting that there is no Cu ion bound in the structure. Diffraction data were collected to 2.5 Å resolution from a flash-cooled crystal at −176 °C at beamline BL5A of the Photon Factory, Japan, and processed with the program suite HKL2000 (Otwinowski and Minor, 1997). The hCutC crystals belong to space group $P\bar{1}$ with unit cell parameters of a = 78.2 Å, b = 78.4 Å, c = 170.4 Å, α = 76.8°, β = 87.9°, and γ = 71.9°, and a solvent content of 59.1%. A summary of the diffraction data statistics is given in

Table 1. We also tried to co-crystallize hCutC with Cu(I) by adding a Cu(I) solution supplemented with DTT either in the protein solution or in the reservoir solution with an ion:protein molar ratio of 10:1. Unfortunately, these attempts were unsuccessful due to the precipitation of the protein.

2.4. Structure determination and refinement

The structure of hCutC was solved by the molecular replacement method with the program CNS (Brunger et al., 1998) using the coordinates of sfCutC (PDB code 1X7I, Zhu et al., 2005) as the search model. Structure refinement was carried out by the program CNS using the standard protocols consisting of conjugate-gradient energy minimization, torsion-constrained molecular dynamics simulated annealing, group *B* factor refinement, and individual *B* factor refinement. Model building was facilitated using the program O (Jones et al., 1991). There are 12 hCutC molecules in the asymmetric unit, forming three dimers of dimers. Thus, strict sixfold non-crystallographic symmetry constraints were applied in the early stage of refinement, but released in the later stage of refinement. A bulk solvent correction and a free *R* factor monitor (calculated with 5% of randomly chosen reflections) were applied throughout the refinement. The stereochemistry quality of the structure model was monitored using the program PROCHECK (Laskowski et al., 1993). The statistics of structure refinement are also summarized in Table 1. Structural analysis was mainly performed using programs in the CCP4 suite (CCP4, 1994). Figures were prepared using the program Pymol (http://www.pymol.org).

Table 1
Summary of diffraction data and structure refinement statistics.

Data collection	
Wavelength (Å)	1.0000
Resolution (Å)	50.0–2.50 (2.59–2.50)[a]
Space group	$P\bar{1}$
Cell parameters	
a, *b*, *c* (Å)	78.2, 78.4, 170.4
α, β, γ (°)	76.8, 87.9, 71.9
Observed reflections	500,939 (50,616)
Unique reflections ($I > 0\sigma(I)$)	127,488 (12,654)
Redundancy	3.9 (4.0)
Mosaicity	0.44
Average I/σ(I)	23.7 (4.1)
Completeness (%)	98.5 (97.9)
R_{merge} (%)[b]	6.0 (29.9)
Refinement	
Number of reflections	127,421
Working set	121,060
Free R set	6361
R_{work} /R_{free} (%)[c]	23.3/28.2
Total number of atoms	22,751
Protein atoms	21,863
Solvent atoms	888
Average *B* factor (Å^2)	56.0
Protein atoms	56.7
Solvent atoms	38.4
RMS deviations	
Bond lengths (Å)	0.011
Bond angles (°)	1.4
Luzzati atomic positional error (Å)	0.37
Ramachandran plot (%)	
Most favored region	89.0
Allowed region	10.7
Generously allowed region	0.3
Disallowed region	0

[a] Values in parentheses refer to the highest resolution shell.
[b] $R_{merge} = \sum_{hkl}\sum_i |I_i(hkl)_i - \langle I(hkl)\rangle| / \sum_{hkl}\sum_i I_i(hkl)$.
[c] $R_{work} = \sum_{hkl} ||F_o| - |F_c|| / \sum_{hkl} |F_o|$.

The coordinates and structure factors of hCutC have been deposited in the RCSB Protein Data Bank with accession code 3IWP.

2.5. Analytical size-exclusion chromatography

The oligomeric state of hCutC in solution was determined by size-exclusion chromatography on a Superdex 200 10/300 column (GE Healthcare). The column was pre-equilibrated with a buffer (20 mM Tris–HCl, pH 8.0, and 100 mM NaCl) and then 200 µl of the hCutC protein (10 mg/ml) was loaded onto the column and eluted with the same buffer at a flow-rate of 0.8 ml/min at 20 °C. Ferritin, aldolase, conalbumin, ovalbumin, and ribonuclease A (LMW Calibration Kit; GE Healthcare) were used to establish a standard curve to determine the apparent molecular weight.

3. Results and discussion

3.1. Copper-binding analysis of hCutC

The previous biological data have suggested that CutC may play an important role in Cu(I) trafficking (Kimura and Nishioka, 1997; Rensing and Grass, 2003). To elucidate the biological function of hCutC, we carried out a biochemical assay on the binding ability of hCutC with Cu(I). The biochemical results show that hCutC is able to bind Cu(I) *in vitro* with a stoichiometry of 1:1 (Fig. 1C), suggesting that hCutC has one Cu-binding site per molecule. The apparent dissociation constant (K_d) was determined to be 15.5 ± 2.8 µM. The binding affinity of hCutC with Cu(I) is much weaker than that of the copper chaperones involved in Cu(I) trafficking which have high binding affinities with the metal ion. For instance, Ctr1, a copper transporter from *Saccharomyces cerevisiae*, exhibits a high binding affinity with Cu(I) ($K_d \approx 10^{-19}$ M) (Xiao et al., 2004). The Cu(I)-responsive transcriptional regulator CueR of *E. coli* can sense Cu(I) in the zeptomolar (10^{-21} M) range (Changela et al., 2003). An Atx1-like copper chaperone CopZ from *Bacillus subtilis* was also reported to have an association constant of $\sim 10^{22}$ M^{-2} (Zhou et al., 2008). The high binding affinity with Cu(I) for these proteins is required by the cells to ensure that there is essentially no free copper in the cells so the copper toxicity is avoided (Rae et al., 1999). In addition, the copper chaperones and copper-transporting proteins are mainly characterized by a X-X-C-X-X-C motif and shared a classical "ferredoxin-like" β-α-β-β-α-β fold (Arnesano et al., 2002). However, these features do not exist in hCutC. Taking these results together, we suggest that hCutC may function as an enzyme with Cu(I) as a cofactor rather than a copper transporter in the trafficking of Cu(I).

3.2. Crystal structure of hCutC

To gain insights into the molecular basis of the potential binding site of hCutC for Cu(I), we determined the crystal structure of hCutC using the molecular replacement method and refined it to 2.5 Å resolution with an *R* factor of 23.3% and a free *R* factor of 28.2% (Table 1). Crystals of hCutC belong to space group $P\bar{1}$ containing 12 hCutC molecules per asymmetric unit. Structure comparison shows no substantial conformational difference among the 12 molecules except some variations in the number of disordered residues at the N- (24–26 residues) and/or C-termini (0–2 residues). The hCutC monomer adopts a typical TIM-barrel $(\beta/\alpha)_8$ fold with an insertion between β8 and α8 which forms two extra β-strands (β9 and β10) linked by a long loop (Fig. 2A). This loop is disordered to varying extent in different molecules, indicating a great flexibility of this region. hCutC shares a 43% sequence identity with sfCutC, and correspondingly the overall structure of hCutC is highly similar to that of sfCutC with a root mean square

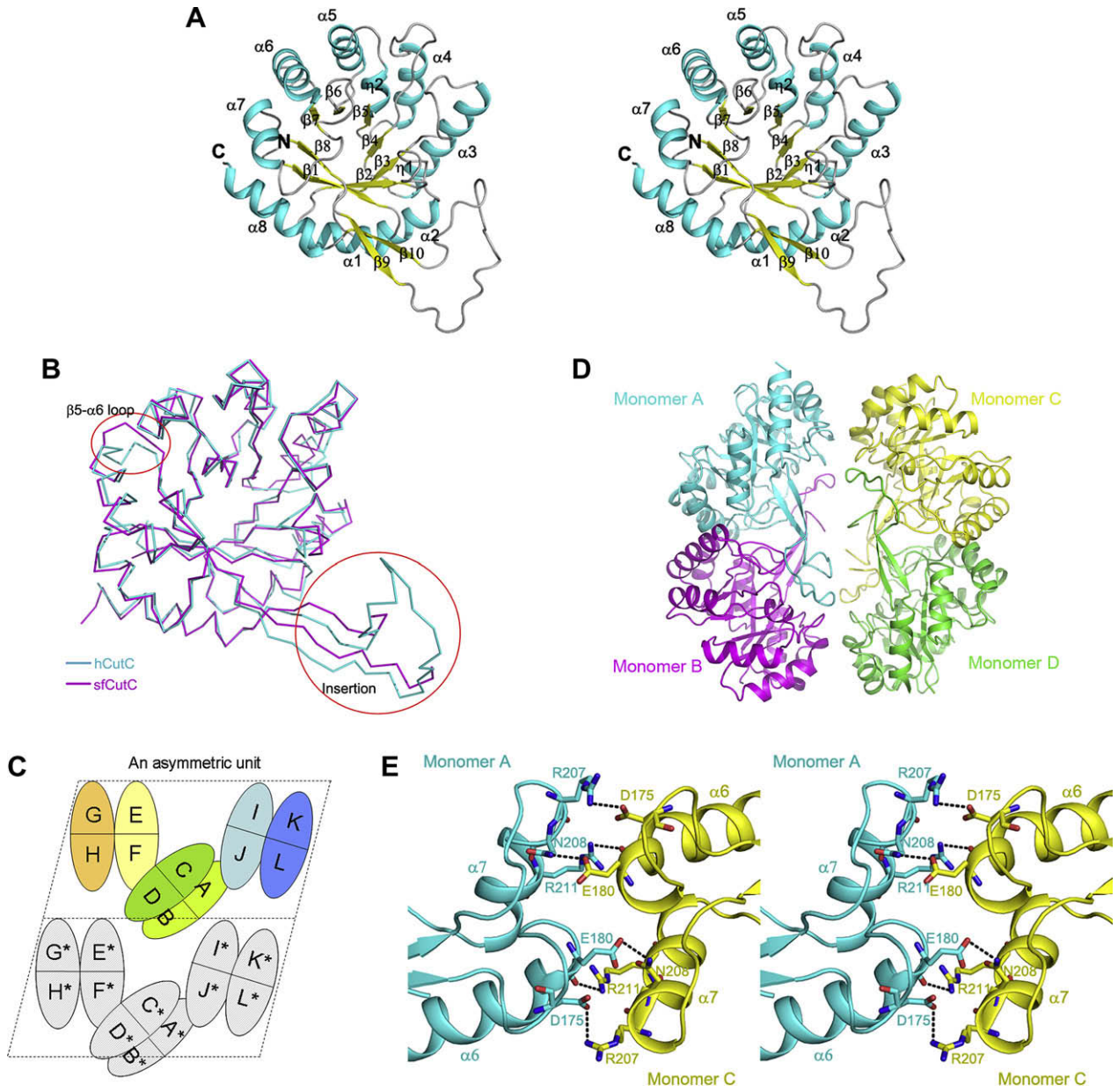

Fig. 2. Crystal structure of hCutC. (A) A stereoview of the hCutC monomer. hCutC assumes a typical TIM-barrel fold with an insertion between β8 and α8 that forms two extra β-strands (β9 and β10) and a long loop. (B) Superposition of hCutC (cyan) with sfCutC (magenta). The regions having large conformational difference are indicated by circles. (C) A schematic diagram showing the crystal packing of the hCutC tetramer in the asymmetric unit. (D) A ribbon diagram showing the tetramer of hCutC. Monomer A is shown in cyan, B in magenta, C in yellow, and D in green. (E) A stereoview showing the hydrogen-bonding interactions between monomers A and C. Residues involved in the interactions are shown with side chains and the hydrogen bonds are indicated with dashed lines.

deviation (RMSD) of 2.6 Å for 210 Cα atoms (Fig. 2B). The major conformational differences reside in the insertion region and the β5-α6 loop. No Cu(I) ion is found to bind to hCutC in the structure, in agreement with the result that no anomalous signal was detected at the wavelength of Cu k-edge in the fluorescence scanning of the crystal at synchrotron. Co-crystallization of hCutC with Cu(I) was unsuccessful due to the precipitation of the protein.

3.3. hCutC exists as a tetramer in both crystal structure and solution

In the crystallographic asymmetric unit, the 12 hCutC molecules form three tetramers (A–D, E–H, and I–L) related by non-crystallographic symmetry (Fig. 2C). Overall, monomers G, H, K, and L have relatively loose packing environments and are not involved in packing contact with other molecules, causing them to have much higher average *B* factors (78.9, 80.6, 81.7, and 91.4 Å^2 for monomers G, H, K, and L, respectively, compared to 56.7 Å^2 for all monomers). The tetramer consists of two dimers and within a tetramer each monomer interacts with two others (Fig. 2D). Monomers A and B form a tight dimer with a buried solvent accessible surface area of 2451 Å^2 or 20.3% for each monomer. There are 16 hydrogen-bonding interactions at this dimer interface (Table 2). Monomers A and C have a loose interface with a buried solvent accessible surface area of 441 Å^2 or 3.6% for each monomer. At this interface, the β6-α6 loop of monomer A interacts with the β7-α7 loop of monomer C via a few hydrophilic interactions, and *vice versa*. Specifically, the side-chain Oδ2 of Asp^{175} of monomer A forms a salt bridge with the side-chain Nη1 of Arg^{207} (2.9 Å) of monomer C. The main-chain carbonyl and side-chain Oε1 of Glu^{180} of monomer A form a hydrogen bond with the side-chain Nη2 of Arg^{211} (3.0 Å)

Table 2
Possible hydrogen bonds between monomers A and B (distance < 3.6 Å).

Monomer A	Monomer B	Distance (Å)
Conserved residues		
Ser63-Oγ	Asp102-Oδ1	2.6
Gly65-N	Asp102-Oδ2	2.9
Asp88-Oδ1	Ser231-Oγ	2.6
Asp102-Oδ1	Gly65-N	2.7
Asp102-Oδ2	Ser63-Oγ	2.6
Asp149-O	Asn237-Nδ2	3.3
Ser231-Oγ	Asp88-Oδ1	2.8
Asn237-Nδ2	Asp149-O	3.2
Not conserved residues		
Tyr109-Oη	Tyr109-Oη	2.9
Glu121-O	Lys234-N	2.9
Glu121-O	Phe235-N	3.0
Asp149-O	Asn237-Nδ2	3.3
Lys234-N	Glu121-O	2.8
Phe235-N	Glu121-O	3.1
Asn237-Nδ2	Cys174-O	3.1
Ala244-N	Ser56-O	2.9

and the side-chain Nδ2 of Asn^{208} (2.9 Å) of monomer C, respectively (Fig. 2E).

In comparison, the crystal structure of sfCutC forms a dimer equivalent to the A/B dimer of hCutC and operation of the crystallographic symmetry could not generate a tetramer similar to that of hCutC. Structural and sequence comparisons show that the residues and interactions involved in the A/B dimer interface are strongly conserved in both hCutC and sfCutC, but the residues involved in the A/C dimer interface are not conserved. Specifically, residues Arg^{207}, Asn^{208}, and Arg^{211} of hCutC that are involved in the formation of the A/C dimer interface correspond to residues Glu^{182}, Asn^{183} and His^{186} of sfCutC, respectively. To investigate whether the tetramer formation of hCutC is due to crystal packing, we analyzed the oligomeric state of hCutC in solution using size-exclusion chromatography. The hCutC molecule is of about 30 kDa determined by the denatured SDS–PAGE of the purified protein which is the same as its theoretic molecular mass (Fig. 1A). However, the apparent molecular weight of the hCutC protein in solution is about 125 kDa (Fig. 1B), suggesting that hCutC exists exclusively as a tetramer in solution as well. We constructed a mutant hCutC containing three mutations R207E/N208A/R211A at the A/C dimer interface which would disrupt the formation of the tetramer and analyzed the oligomeric state of the mutant. The size-exclusion chromatography result shows that as expected, the mutant hCutC exists as a dimer in solution (data not shown). These results indicate that the tetramer formation appears to be a unique feature of hCutC; however, its biological implication is unclear.

3.4. A potential Cu(I)-binding site

The previous sequence analysis of several bacterial CutC proteins reveals a conserved sequence motif of M-X-X-M-X-X-X-M (Odermatt et al., 1993). By analogy to the putative Cu-binding motif of M-X-X-X-X-M-X-X-M in the CopB ATPase from *Enterococcus hirae*, this sequence motif is suggested to be a Cu-binding motif and the conserved Met residues are involved in Cu-binding (Odermatt et al., 1993). However, further sequence comparison of the CutC proteins from both bacteria and eukaryotes indicates that this sequence motif is not conserved (Fig. 3A). Moreover, in the sfCutC structure this sequence motif is located on α4, and the Met residues orient their side chains towards the protein core formed by several hydrophobic residues (Val^{94}, Val^{101}, Val^{118}, Phe^{120}, Leu^{137}, Leu^{140}, and Ile^{142}) and therefore are solvent inaccessible (Zhu et al., 2005). Together, the solvent inaccessibility and the hydrophobic environment of the Met residues indicate that this sequence motif is very unlikely to form part of a Cu-binding site.

On the other hand, structural analysis of hCutC shows that there are two Cys residues (Cys^{31} and Cys^{52}) at the C-terminal ends of β1 and β2 which are exposed to the inner surface of the TIM-barrel and are solvent accessible (Fig. 3B and C). These two Cys residues are strictly conserved in all identified CutC proteins from various species. The two Cys residues form a disulfide bond in the structure of hCutC. In the structure of sfCutC, the distance between the thiol groups of the corresponding Cys^{7} and Cys^{28} is 4.1 Å (Zhu et al., 2005), which is appropriate for binding of a Cu(I) ion. The TIM-barrel fold is a common framework for many enzymes and the active sites of these enzymes are always located at the C-terminal ends of the β-strands (Wierenga, 2001). Additionally, many Cu(I)-binding proteins bind Cu(I) with a low coordination number and in a solvent accessible environment (Finney and O'Halloran, 2003). Thus, we propose that hCutC and other CutC proteins might function as an enzyme with Cu(I) as a cofactor and the two Cys residues of the CutC proteins may be involved in the Cu(I)-binding by constituting part of the Cu(I)-binding site. To investigate this possibility, we mutated the two Cys residues to Ala and examined their respective effects on the binding ability of hCutC with Cu(I). As shown in Fig. 1D, the binding abilities (the $[\text{Cu-hCutC}]/[\text{hCutC}]_{\text{tot}}$ ratio) of the single mutants C31A and C52A and the double mutant C31A/C52A for the Cu(I) ion were significantly reduced to about 36%, 46%, and 26% of that of the wild-type hCutC, respectively. These results further support our notion that both Cys^{31} and Cys^{52} play a critical role in the Cu-binding. Nevertheless, since the mutants retained some binding ability, it is likely that in addition to the two Cys residues, some other residues in the vicinity may also participate in the Cu-binding.

To further investigate the possibility of whether the two conserved Cys residues could form part of a potential Cu(I)-binding site, we compared the Cu(I)-binding sites of different Cu(I)-binding proteins to see if there is any structural conservation and similarity. The results show that Cu(I) prefers to be coordinated by soft ligands such as sulfhydryl group with a coordination number of 2, 3, or 4. In copper chaperones, Cu(I) is usually coordinated by two cysteines and delivered to another protein by forming a Cu-$(\text{S-Cys})_3$ intermediate (Huffman and O'Halloran, 2001). However, CsoR, a copper-sensing transcriptional regulator, binds copper with two cysteines and one histidine (Liu et al., 2007). Moreover, in the enzyme CODH/ACS (carbon monoxide dehydrogenase/acetyl-CoA synthase), Cu(I) functions as a cofactor and is coordinated by three cysteines (Doukov et al., 2002). It appears that similar binding modes can exist in proteins with different functions and thus it is hard to gain useful information about whether hCutC functions as a transporter or an enzyme through comparison of the copper-binding sites. On the other hand, it is evident that the Cu(I)-binding site of these Cu(I)-binding proteins is composed of two Cys residues and possibly some other residue(s). Our biochemical results are in agreement with this observation, which suggest that the Cu(I)-binding site of hCutC may consist of two Cys residues (Cys^{31} and Cys^{52}) and possibly other conserved residues in the vicinity. Although the two Cys residues form a disulfide bond in the current structure, it is possible that in the presence of a Cu(I) ion, the disulfide bond of hCutC might be broken and subsequently the two Cys residues would bind to the Cu(I) ion. A similar case is seen in the structures of Atx1 which is a copper chaperone that functions in shuttling Cu(I) to the transport ATPase Ccc2. Cys^{15} and Cys^{18} of Atx1 form a disulfide bridge in the apo-form Atx1, but bind to an Hg ion that mimics a Cu(I) ion in the structure of the Atx1–Hg complex (Rosenzweig et al., 1999).

Structural analysis of the putative Cu(I)-binding site of hCutC reveals that on the inner surface of the TIM-barrel near the two

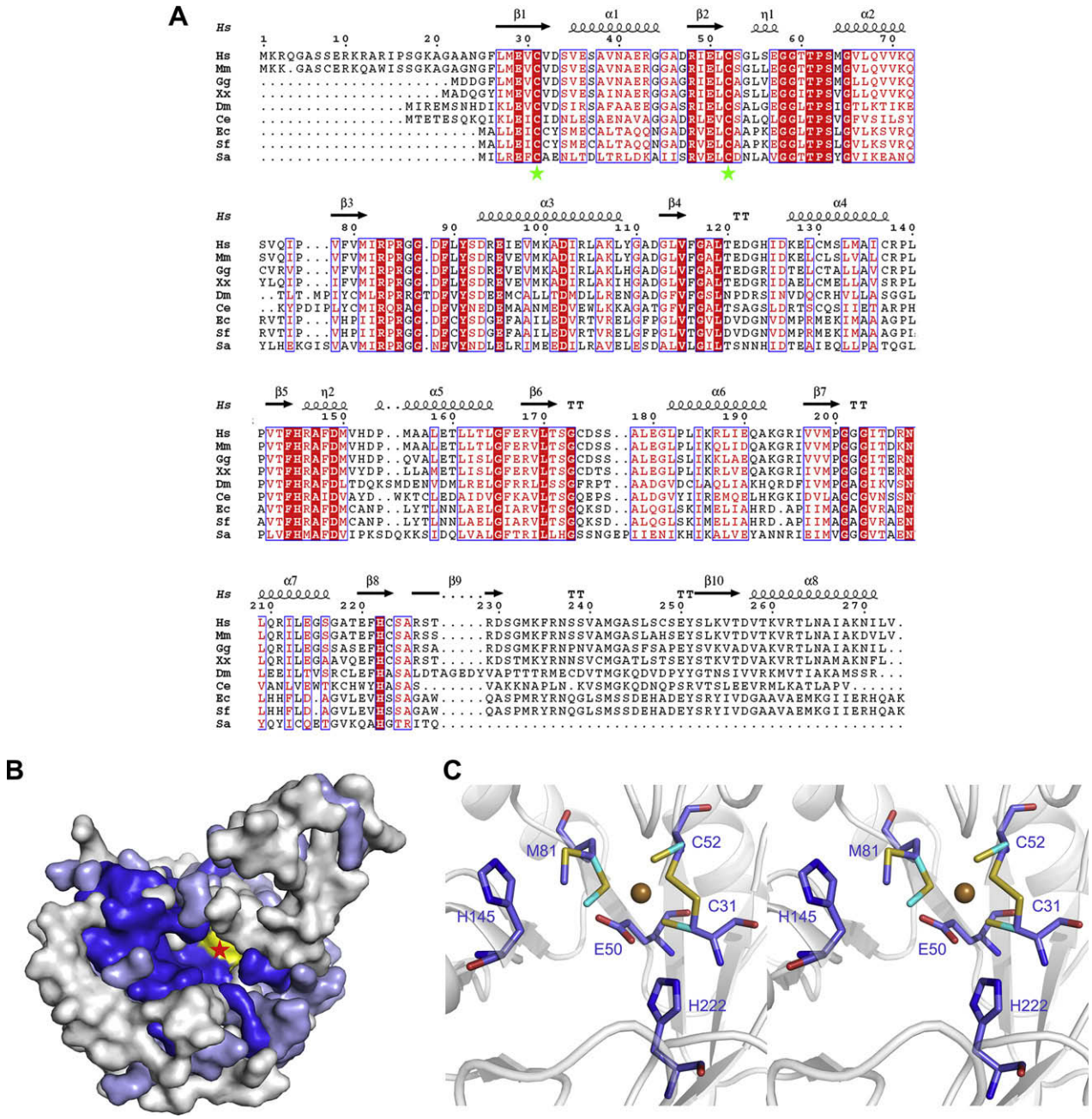

Fig. 3. A potential Cu(I)-binding site of hCutC. (A) Structure-based sequence alignment of CutC from different species. Hs, *Homo sapiens*; Mm, *Mus musculus*; Gg, *Gallus gallus*; Xx, *Xenopus tropicalis*; Dm, *Drosophila melanogaster*; Ce, *Caenorhabditis elegans*; Ec, *Escherichia coli*; Sf, *Shigella flexneri*; and Sa, *Streptococcus agalactiae*, respectively. Strictly conserved residues are highlighted in shaded red boxes and conserved residues in open red boxes. The secondary structures of hCutC are shown above the alignment. The alignment was generated using ESPript (Gouet et al., 1999). (B) A molecular surface of hCutC showing the location of the potential Cu(I)-binding site. The potential Cu(I)-binding site which is marked with a red star is located on the inner surface of the C-terminal end of the TIM-barrel. The two strictly conserved Cys^{31} and Cys^{52} at the putative binding site are colored in yellow. The strictly and highly conserved residues are colored in blue and light-blue, respectively. (C) A stereoview of the putative Cu(I)-binding site of hCutC. The side chains of the conserved residues forming the putative Cu(I)-binding site are shown in blue ball-and-stick models. The side chains of residues Cys^{31} and Cys^{52} in reduced form and residue Met^{81} in a different rotamer are shown in cyan ball-and-stick models. A modeled Cu(I) ion is shown with a gold ball.

Cys residues there are several highly conserved residues including Glu^{50}, Met^{81}, His^{145}, and His^{222} (Fig. 3C). Modeling studies show that with a proper rotation the side chain of Met^{81} could be positioned with favorable distance and angle to bind a metal ion together with Cys^{31} and Cys^{52}. His^{145} is positioned about 8 Å away from the putative Cu(I)-binding site in the current structure. However, since it is located in the β5-η2 loop which has a relatively greater flexibility, His^{145} could also be a potential ligand for Cu(I)-binding if a proper conformational change could take place upon the metal binding. In addition, Glu^{50} and His^{222} might be involved in the stabilization of the Cu(I)-binding site. Unfortunately, mutations of these residues led to either poor expression or aggregation of the recombinant proteins, and thus we could not validate their effects on the binding ability of hCutC with Cu(I).

4. Conclusion

CutC is a family of proteins conserved from bacteria to mammals that have been implicated to play an important role in the

intracellular trafficking of Cu(I). However, the exact biological function of CutC is unclear. We have analyzed the copper-binding ability and determined the crystal structure of hCutC. The biochemical data show that hCutC can bind Cu(I) with a stoichiometry of 1:1 and a relatively low binding affinity (K_d = 15.5 ± 2.8 μM). hCutC adopts a typical TIM-barrel fold and exists as a tetramer in both crystal structure and solution which is different from the dimeric assembly of the bacterial orthologs. Structural analysis and sequence comparison of CutC from different species reveal two strictly conserved Cys residues Cys^{31} and Cys^{52} and several highly conserved polar residues on the inner surface of the C-terminal end of the TIM-barrel. Mutations of these two Cys residues can significantly decrease the copper-binding ability of hCutC. Collectively, these results provide important insights into the biological function of hCutC by suggesting a potential function of hCutC as an enzyme involved in copper homeostasis using Cu(I) as a cofactor rather than a copper transporter and the putative Cu(I)-binding site consisting of the conserved Cys^{31} and Cys^{52} and other conserved residues in the vicinity.

Acknowledgments

We thank the staff members at Photon Factory, Japan for support in diffraction data collection and other members of our group for helpful discussion. This work was supported by grants from the Ministry of Science and Technology of China (2006AA02A313 and 2007CB914302), the National Natural Science Foundation of China (30730028), the Chinese Academy of Sciences (KSCX2-YW-R-107 and SIBS2008002), and the Science and Technology Commission of Shanghai Municipality (07XD14032).

References

Arnesano, F., Banci, L., Bertini, I., Ciofi-Baffoni, S., Molteni, E., Huffman, D.L., O'Halloran, T.V., 2002. Metallochaperones and metal-transporting ATPases: a comparative analysis of sequences and structures. Genome Res. 12, 255–271.

Bradford, M.M., 1976. A rapid and sensitive method for the quantitation of microgram quantities of protein utilizing the principle of protein–dye binding. Anal. Biochem. 72, 248–254.

Brunger, A.T., Adams, P.D., Clore, G.M., DeLano, W.L., Gros, P., Grosse-Kunstleve, R.W., Jiang, J.S., Kuszewski, J., Nilges, M., Pannu, N.S., Read, R.J., Rice, L.M., Simonson, T., Warren, G.L., 1998. Crystallography & NMR system: a new software suite for macromolecular structure determination. Acta Crystallogr. D 54, 905–921.

Calafato, S., Swain, S., Hughes, S., Kille, P., Sturzenbaum, S.R., 2008. Knockdown of *Caenorhabditis elegans* cutc-1 exacerbates the sensitivity towards high levels of copper. Toxicol. Sci. 106, 7.

CCP4, 1994. The CCP4 suite: programs for protein crystallography. Acta Crystallogr. D 50, 760–763.

Changela, A., Chen, K., Xue, Y., Holschen, J., Outten, C.E., O'Halloran, T.V., Mondragon, A., 2003. Molecular basis of metal-ion selectivity and zeptomolar sensitivity by CueR. Science 301, 1383–1387.

DiDonato, M., Sarkar, B., 1997. Copper transport and its alterations in Menkes and Wilson diseases. Biochim. Biophys. Acta 1360, 3–16.

Doukov, T.I., Iverson, T.M., Seravalli, J., Ragsdale, S.W., Drennan, C.L., 2002. A Ni–Fe–Cu center in a bifunctional carbon monoxide dehydrogenase/acetyl-CoA synthase. Science 298, 567–572.

Finney, L.A., O'Halloran, T.V., 2003. Transition metal speciation in the cell: insights from the chemistry of metal ion receptors. Science 300, 931–936.

Gouet, P., Courcelle, E., Stuart, D.I., Metoz, F., 1999. ESPript: analysis of multiple sequence alignments in PostScript. Bioinformatics 15, 305–308.

Gupta, S.D., Lee, B.T., Camakaris, J., Wu, H.C., 1995. Identification of cutC and cutF (nlpE) genes involved in copper tolerance in *Escherichia coli*. J. Bacteriol. 177, 4207–4215.

Huffman, D.L., O'Halloran, T.V., 2001. Function, structure, and mechanism of intracellular copper trafficking proteins. Annu. Rev. Biochem. 70, 677–701.

Jensen, P.Y., Bonander, N., Horn, N., Tumer, Z., Farver, O., 1999. Expression, purification and copper-binding studies of the first metal-binding domain of Menkes protein. Eur. J. Biochem. 264, 890–896.

Jones, T.A., Zou, J.Y., Cowan, S.W., Kjeldgaard, M., 1991. Improved methods for building protein models in electron density maps and the location of errors in these models. Acta Crystallogr. A 47, 110–119.

Kimura, T., Nishioka, H., 1997. Intracellular generation of superoxide by copper sulphate in *Escherichia coli*. Mutat. Res. 389, 237–242.

Laskowski, R.A., Macarthur, M.W., Moss, D.S., Thornton, J.M., 1993. Procheck—a program to check the stereochemical quality of protein structures. J. Appl. Crystallogr. 26, 283–291.

Lee, J., Prohaska, J.R., Thiele, D.J., 2001. Essential role for mammalian copper transporter Ctr1 in copper homeostasis and embryonic development. Proc. Natl. Acad. Sci. USA 98, 6842–6847.

Li, J., Ji, C., Chen, J., Yang, Z., Wang, Y., Fei, X., Zheng, M., Gu, X., Wen, G., Xie, Y., Mao, Y., 2005. Identification and characterization of a novel Cut family cDNA that encodes human copper transporter protein CutC. Biochem. Biophys. Res. Commun. 337, 179–183.

Liu, T., Ramesh, A., Ma, Z., Ward, S.K., Zhang, L., George, G.N., Talaat, A.M., Sacchettini, J.C., Giedroc, D.P., 2007. CsoR is a novel *Mycobacterium tuberculosis* copper-sensing transcriptional regulator. Nat. Chem. Biol. 3, 60–68.

Mao, M., Fu, G., Wu, J.S., Zhang, Q.H., Zhou, J., Kan, L.X., Huang, Q.H., He, K.L., Gu, B.W., Han, Z.G., Shen, Y., Gu, J., Yu, Y.P., Xu, S.H., Wang, Y.X., Chen, S.J., Chen, Z., 1998. Identification of genes expressed in human CD34(+) hematopoietic stem/progenitor cells by expressed sequence tags and efficient full-length cDNA cloning. Proc. Natl. Acad. Sci. USA 95, 8175–8180.

Odermatt, A., Suter, H., Krapf, R., Solioz, M., 1993. Primary structure of two P-type ATPases involved in copper homeostasis in *Enterococcus hirae*. J. Biol. Chem. 268, 12775–12779.

Ota, T., Suzuki, Y., Nishikawa, T., Otsuki, T., Sugiyama, T., Irie, R., Wakamatsu, A., Hayashi, K., Sato, H., Nagai, K., et al., 2004. Complete sequencing and characterization of 21, 243 full-length human cDNAs. Nat. Genet. 36, 40–45.

Otwinowski, Z., Minor, W., 1997. Processing of X-ray diffraction data collected in oscillation mode. Methods Enzymol. 276, 307–326.

Pena, M.M., Lee, J., Thiele, D.J., 1999. A delicate balance: homeostatic control of copper uptake and distribution. J. Nutr. 129, 1251–1260.

Rae, T.D., Schmidt, P.J., Pufahl, R.A., Culotta, V.C., O'Halloran, T.V., 1999. Undetectable intracellular free copper: the requirement of a copper chaperone for superoxide dismutase. Science 284, 805–808.

Rensing, C., Grass, G., 2003. *Escherichia coli* mechanisms of copper homeostasis in a changing environment. FEMS Microbiol. Rev. 27, 197–213.

Rosenzweig, A.C., Huffman, D.L., Hou, M.Y., Wernimont, A.K., Pufahl, R.A., O'Halloran, T.V., 1999. Crystal structure of the Atx1 metallochaperone protein at 1.02 Å resolution. Structure 7, 605–617.

Schaefer, M., Gitlin, J.D., 1999. Genetic disorders of membrane transport. IV. Wilson's disease and Menkes disease. Am. J. Physiol. 276, G311–G314.

Silver, S., Phung, L.T., 1996. Bacterial heavy metal resistance: new surprises. Annu. Rev. Microbiol. 50, 753–789.

Wierenga, R.K., 2001. The TIM-barrel fold: a versatile framework for efficient enzymes. FEBS Lett. 492, 193–198.

Xiao, Z., Loughlin, F., George, G.N., Howlett, G.J., Wedd, A.G., 2004. C-terminal domain of the membrane copper transporter Ctr1 from *Saccharomyces cerevisiae* binds four Cu(I) ions as a cuprous-thiolate polynuclear cluster: sub-femtomolar Cu(I) affinity of three proteins involved in copper trafficking. J. Am. Chem. Soc. 126, 3081–3090.

Zhou, L., Singleton, C., Le Brun, N.E., 2008. High Cu(I) and low proton affinities of the CXXC motif of *Bacillus subtilis* CopZ. Biochem. J. 413, 459–465.

Zhu, D.Y., Zhu, Y.Q., Huang, R.H., Xiang, Y., Yang, N., Lu, H.X., Li, G.P., Jin, Q., Wang, D.C., 2005. Crystal structure of the copper homeostasis protein (CutCm) from *Shigella flexneri* at 1.7 Å resolution: the first structure of a new sequence family of TIM barrels. Proteins 58, 764–768.